34th Annual International Conference of the IEEE EMBS
San Diego, California USA, 28 August - 1 September, 2012

The relationship between transcranial Current Stimulation electrode montages and the effect of the skull orbital openings

A. Mekonnen, R. Salvador, G. Ruffini, P. C. Miranda

Abstract— **Due to its low electric conductivity, the skull has a major impact on the electric field distribution in the brain in transcranial current stimulation (tCS). However, the skull has several openings that are filled with higher conductivity soft tissues, and through which a significant fraction of the injected current may pass. We show that current entering the brain via the orbital openings increases the electric field intensity in the cortical regions near the orbit. Furthermore, this depends on the how far electrodes are placed from the orbital openings.**

I. Introduction

Transcranial current stimulation (tCS) is a noninvasive brain stimulation technique in which a weak DC or slowly varying electrical current is applied to the brain through the scalp. tCS is capable of eliciting neural excitability changes in the human cortex ([1], [2]). The level of neural modulation by tCS depends on the strength of the induced electric field/current density in the brain and on many other factors, such as the properties of the stimulated neurons or their orientation relative to the electric field.

Only a fraction of the current applied in tCS enters the brain as much of it is shunted through the scalp due to the relative low conductivity of the skull ([5]). However, some current may reach the brain through the skull openings. The human skull has several openings through which soft tissues such as nerves and vessels enter the cranial cavity. Due to the higher electric conductivity of soft tissues, current may pass through these openings during tCS and affect the electric field in the cortex. The superior orbital fissure and optical foramen are such openings to be found near the apex of the orbit. The shape and surface area of the orbital fissures vary considerably among individuals ([3]). The total area of the superior orbital fissure and optic foramen is approximately 1 cm^2 ([3], [4]). We used a realistic human head model based on the finite element method to simulate tCs in order to investigate the effect of skull openings on the electric field in the cortex.

The intensity of the current entering through the skull openings depends on how far the stimulation electrodes are placed from the apertures. Thus, we considered various electrode configurations in order to compare the current density at the orbital openings.

In 2008, Kanai et al. used transcranial alternating current stimulation (tACS) to show that stimulation of the visual cortex induced phosphenes in a frequency dependent manner ([6]). Their claim has since been a subject of debate among researchers in which they argue that the retina, and not the visual cortex, is responsible for phosphene induction ([7], [8]). Our realistic head model does yet not include an accurate representation of the eye, so we cannot precisely predict the electric field intensity in the retina. Instead, we show the impact of the position of the electrodes relative to the skull openings on the electric field in the brain.

II. Methods

A realistic finite element model of the human head was generated based on MR images with an isotropic resolution of 1 mm ([9]). The model consisted of the five major tissues of the head: white matter, gray matter, cerebrospinal fluid (CSF, including the ventricles), skull and scalp. In addition, cylindrical sub-domains with a cross-sectional area of 1 cm^2 representing the orbital openings were included in the model, as it was not possible to segment the individual openings in these images. The cylinders link the scalp to the CSF and are shown in fig. 1, approximately at the apexes of the orbits.

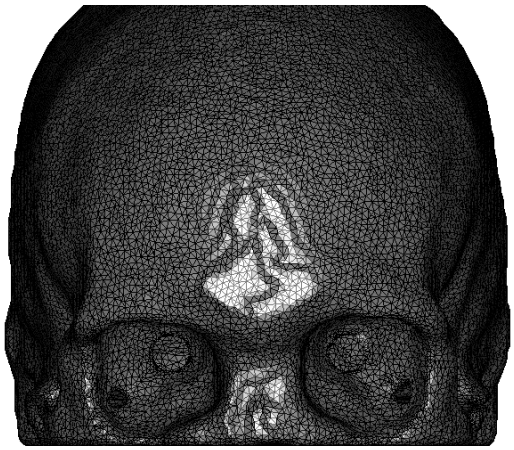

Figure 1. The skull mesh with cylindrical holes at the apexes of the orbits.

The following Finite Element models were generated, corresponding to three different electrode configurations. For each configurations we also considered a model without the presence of orbital openings in order to study their effect on the electric field distribution in the brain. The conductivity of the sub-domains representing the openings were set to equal that of: (a) the skull, i.e., no openings, (b) the scalp, i.e., openings filled with soft tissues are present.

The project HIVE acknowledges the financial support of the Future and Emerging Technologies (FET) programme within the Seventh Framework Programme for Research of the European Commission, under FET-Open grant number: 222079.

A. Mekonnen and R. Salvador, and are with the Institute of Biophysics and Biomedical Engineering (IBEB), Faculty of Sciences, University of Lisbon, 1749-016 Lisbon, Portugal (phone: +351217500177; fax: +351217500030; e-mail: aamekonnen@fc.ul.pt). G. Ruffini is with Starlab, Barcelona, Spain. P. C. Miranda is with Neuroelectrics, Barcelona, Spain.

A. Electrode configuration 1

Two 35 cm^2 rectangular electrodes were placed as in typical motor cortex stimulation experiments ([10]): the anode was placed over the motor cortex and the cathode above the contra lateral eyebrow, as shown in fig. 2.

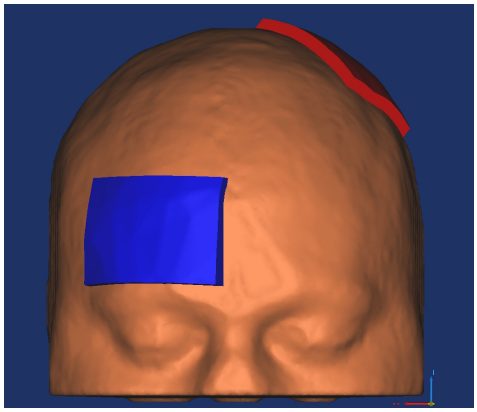

Figure 2. Front view of the head model with electrode configuration 1: cathode in blue, anode in red.

B. Electrode configuration 2

The electrode montage used for visual cortex stimulation in ([6]) was modelled. A 9x6 cm^2 cathode was placed at Cz whilst a 4x3 cm^2 anode was placed at Oz (10/10 International System), as shown in fig. 3.

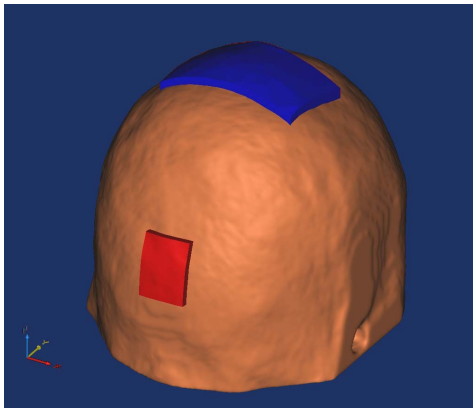

Figure 3. View of the head model with electrode configuration 2: cathode in blue, anode in red.

C. Electrode configuration 3

A 1 cm radius (π cm^2) anode was placed at C3 and 4 cathodes of the same size were placed at AF8, AF7, PO7 and PO8, see fig. 4. The aim of this montage was to create a single high electric field region in the cortex under the anode with weaker electric field regions under the cathodes. The use of several smaller return electrodes is likely to be more effective than a single large electrode in reducing the electric field under the return electrode(s) ([11]).

In all montages a current of 1 mA was injected through the anode. In the last configuration, the return current was divided equally among the 4 cathodes.

All calculations were performed in COMSOL (http://www.comsol.com), using its Conductive Media DC package. This package solves Poisson's equation and allows for the calculation of the electric potential. Once the electric potential is known, its gradient yields the electric field.

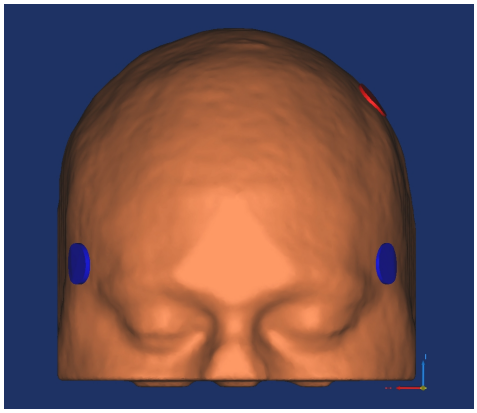

Figure 4. Front view of the head model with electrode configuration 3: cathodes in blue, anode in red.

Given the large number of degrees of freedom in the model (more than 5×10^6), an iterative linear system solver (GMRES) was chosen. This iterative solver required that a pre-conditioner be used (Incomplete LU with a drop tolerance of 0.005). The calculation took less than 3 hours to complete in a workstation with a quad-core Core i7-860 CPU and 16 GB of RAM.

III. Results

The following three figures show the magnitude of the electric field on the cortical surface in the gray matter with the openings present (top) and the magnitude of the difference of the electric field with and without openings (bottom). The solution was smoothed on this boundary to avoid spurious extreme values.The viewpoint was chosen so as to show clearly the electric field in the region behind the orbital openings, particularly the temporal poles and the orbitofrontal cortex. The range of the scale for the electric field plots (top) was set to 0 - 0.21 V/m in all configurations to make comparisons easier.

For electrode configuration 1, the magnitude of the electric field with the orbital openings present is shown in fig. 5a. With the inclusion of openings, the local maximum at the right temporal pole increased from 0.13 V/m to 0.18 V/m whereas the maximum in the right orbitofrontal field decreased slightly from 0.21 to 0.20 V/m. The global maximum of the electric field magnitude was 0.38 V/m and was located at the bottom of a sulcus near the anode. The magnitude of the difference of the electric field with and without the openings, shown in fig. 5b, is large because the presence of the openings shifts the local electric field maximum in the temporal pole to a nearby position where the field was low in the absence of the openings.

The electric field on the gray matter surface for electrode configuration 2 is shown in fig. 6. It is practically the same with or without the orbital openings and it is almost symmetric. The maximum values at the temporal poles and in the orbitofrontal cortices are about 0.06 V/m in both cases. The global maximum of the electric field magnitude is 0.84 V/m and is located under the anode, pinned to a narrowing in

the interhemispheric fissure. The maximum magnitude of the difference in the electric field is less than 0.01 V/m and is located at the temporal pole. Note that the range of the scale for the difference plots was decreased to 0 - 0.1 V/m in the next two figures.

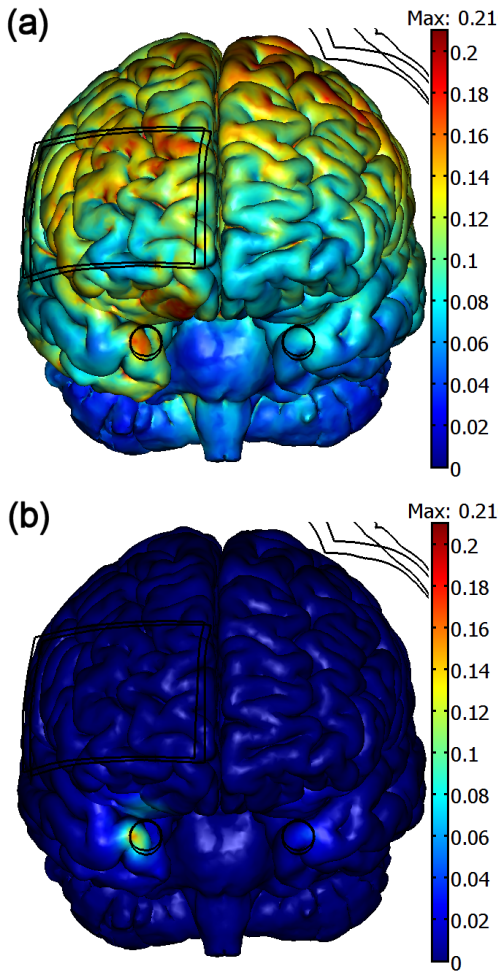

Figure 5. (a) Magnitude of the electric field (V/m) on the gray matter surface for electrode configuration 1, with the orbital openings. (b) Magnitude of the difference of the electric field with and without openings. The cylinders representing the orbital apertures are clearly visible.

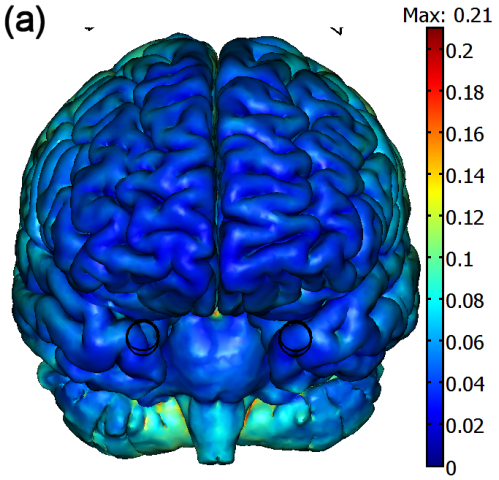

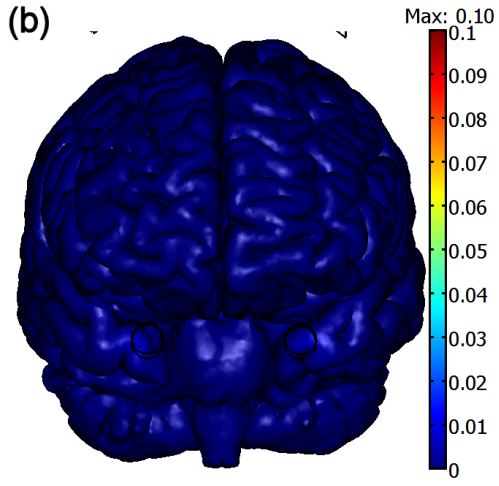

Figure 6. (a) Magnitude of the electric field (V/m) on the gray matter surface for electrode configuration 2, with the orbital openings. (b) Magnitude of the difference of the electric field with and without openings.

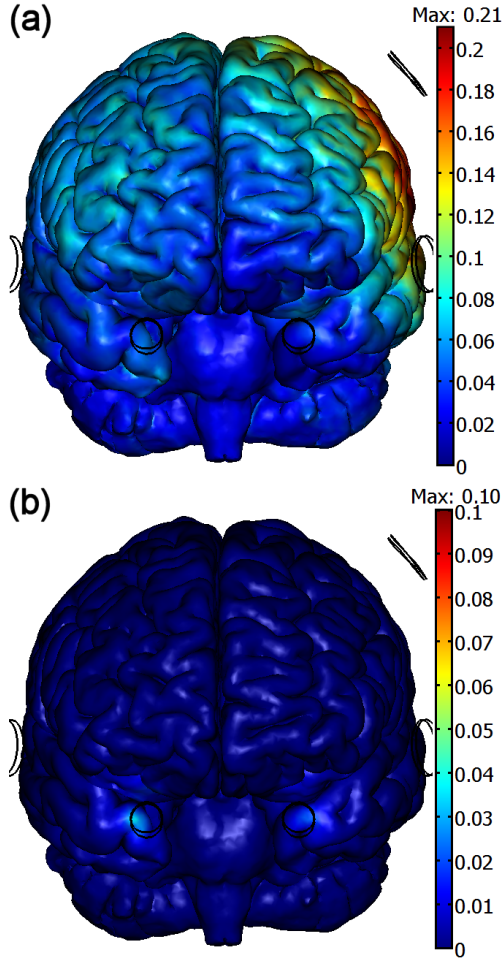

Figure 7. (a) Magnitude of the electric field (V/m) on the gray matter surface for electrode configuration 3, with the orbital openings. (b) Magnitude of the difference of the electric field with and without openings.

The electric field for electrode configuration 3 is shown in fig. 7. There is a slight increase in the maximum value of the electric field in the temporal poles and the right orbitofrontal cortex but the maximum values remain approximately equal to 0.06 V/m in both figures. The extent of these high field regions also increases slightly. The global

maximum of the electric field magnitude is 0.48 V/m. It occurs under the anode because the current through this electrode is higher than through the others. The maximum magnitude of the difference in the electric field is less than 0.04 V/m and is also located at the temporal pole.

In order to quantify the current entering the brain through the orbital apertures, the normal component of the current density was integrated over the orbital aperture boundary surface that is in contact with the CSF. The results are shown in table I. In the case of tDCS, the current flows out of the cranium in the three configurations studied. This is because the electrode nearest to the opening was always a cathode.

TABLE I. CURRENT PASSING THROUGH THE POSTERIOR BOUNDARY OF THE ORBITAL OPENINGS, IN μA.

Configuration	Left orbit	Right orbit
1(a) – no openings	0.6	1.7
1(b) – with openings	11.1	30.9
2(a) – no openings	1.0	1.2
2(b) – with openings	1.5	1.6
3(a) – no openings	0.4	0.4
3(b) – with openings	6.4	7.9

IV. DISCUSSION

Our modeling study shows that the existence of skull openings has a moderate impact on the electric field in the cortex near the opening. This happens only if one of the electrodes is placed near the opening. In the case of configuration 1, used for stimulation of the motor cortex, the field at the temporal pole increases by almost 50% due to the presence of the apertures, from 0.13 V/m to 0.18 V/m. The change in the electric field in the cortex near the orbital opening is negligible in the other two montages.

In configuration 1, the strength of the electric field in the right orbitofrontal cortex is practically independent of the existence of the opening. Instead, it depends on the size and the position of the electrode in the supraorbital region. In this configuration, the electric field in the right orbitofrontal cortex reaches about 50% of the absolute maximum.

Configuration 2 produces a low electric field in the cortex near the orbital openings and has the lowest current flowing through those openings. This suggests that the electric field in the retina may be low too, however stimulation of the retina cannot be excluded due to its lower stimulation threshold. A more detailed model of the eye and surrounding tissues (e.g., [12]) is required to determine whether stimulation is occurring at the visual cortex or at the retina when using this configuration for tCS.

One of the benefits of using several return electrodes is demonstrated in configuration 3. Despite the fact that small electrodes are placed near the orbital opening, the impact on the electric field in the nearby cortex is limited, due to the fact that only one quarter of the injected current returns through each one of these electrodes. Thus the use of multiple return electrodes allows placing them near skull openings.

The amount of current passing through the openings is small but represents a significant fraction of the injected current considering that the skull in our model has an inner total area of 860 cm^2 and the openings have a total cross-sectional area of 2 cm^2. In the case of configuration 1, about 4% of the injected current passes through openings that represent only 0.25% of the skull's area. Also, the effect on the electric field in the cortex increases gradually with the current passing through the apertures. The effect is practically absent when the current through each opening is about 1 μA, it becomes visible when the current reaches around 10 μA and is evident when the current reaches 30 μA. The effect is likely to depend on the shape of the cortex in the vicinity of the opening.

In conclusion, the natural skull openings at the back of the orbit have a moderate impact on the electric field in the cortex near them when one electrode in a bipolar montage is placed near the opening. Thus, in the configuration normally used for stimulation of the motor cortex, the presence of the openings lead to an increase in the electric field magnitude of about 50% in the temporal pole. Also, a significant electric field is produced in the orbitofrontal cortex, independently of the openings. However, in the other montages studied these effects were negligible.

REFERENCES

[1] Ardolino G, Bossi B, Barbieri S, Priori A. Non-synaptic mechanisms underlie the after-effects of cathodal transcutaneous direct current stimulation of the human brain. *J Physiol*. 2005;568(Pt2):653-63.

[2] Nitsche MA, Seeber A, Frommann K, et al. Modulating parameters of excitability during and after transcranial direct current stimulation of the human motor cortex. *J Physiol*. 2005;568(Pt 1):291-303.

[3] Reymond J, Kwiatkowski J, Wysocki J. Clinical anatomy of the superior orbital fissure and the orbital apex. *J Craniomaxillofac Surg*. 2008;36(6):346-53.

[4] Fujiwara T, Matsuda K, Kubo T, Tomita K, Yano K, Hosokawa K. Superior orbital fissure syndrome after repair of maxillary and naso-orbito-ethmoid fractures: a case study. *J Plast Reconstr Aesthet Surg*. 2009;62(12):565-9.

[5] Miranda PC, Lomarev M, Hallett M. Modeling the current distribution during transcranial direct current stimulation. *Clin Neurophysiol*. 2006;117(7):1623-9.

[6] Kanai R, Chaieb L, Antal A, Walsh V, Paulus W. Frequency-dependent electrical stimulation of the visual cortex. *Curr Biol*. 2008;18(23):1839-43.

[7] Schwiedrzik CM. Retina or visual cortex? The site of phosphene induction by transcranial alternating current stimulation. *Front Integr Neurosci*. 2009;3:6.

[8] Schutter DJ, Hortensius R. Retinal origin of phosphenes to transcranial alternating current stimulation. *Clin Neurophysiol*. 2010;121(7):1080-4.

[9] Salvador R, Mekonnen A, Ruffini G, Miranda PC. Modeling the electric field induced in a high resolution realistic head model during transcranial current stimulation. *32nd Annual International Conference of the IEEE Engineering in Medicine and Biology Society*. 2010;1:2073-6.

[10] Nitsche MA, Boggio PS, Fregni F, Pascual-Leone A. Treatment of depression with transcranial direct current stimulation (tDCS): a review. *Exp Neurol*. 2009;219(1):14-9.

[11] Faria P, Hallett M, Miranda PC. A finite element analysis of the effect of electrode area and inter-electrode distance on the spatial distribution of the current density in tDCS. *J Neural Eng*. 2011;8: 066017.

[12] Lindenblatt G, Silny J. A model of the electrical volume conductor in the region of the eye in the ELF range. *Phys Med Biol*. 2001;46:3051-9.